Flat field concave holographic grating with broad spectral region and moderately high resolution

Jian Fen Wu,[1,*] Yong Yan Chen,[1] and Tai Sheng Wang[2]

[1]Central Institute of Iron & Steel Research, Beijing 100081, China

[2]Changchun Institute of Optics, Fine Mechanics and Physics, Chinese Academy of Sciences, Changchun 130033, China

*Corresponding author: wjf_85@163.com

Received 10 August 2011; revised 17 October 2011; accepted 17 October 2011; posted 18 October 2011 (Doc. ID 152522); published 27 January 2012

In order to deal with the conflicts between broad spectral region and high resolution in compact spectrometers based on a flat field concave holographic grating and line array CCD, we present a simple and practical method to design a flat field concave holographic grating that is capable of imaging a broad spectral region at a moderately high resolution. First, we discuss the principle of realizing a broad spectral region and moderately high resolution. Second, we provide the practical method to realize our ideas, in which Namioka grating theory, a genetic algorithm, and ZEMAX are used to reach this purpose. Finally, a near-normal-incidence example modeled in ZEMAX is shown to verify our ideas. The results show that our work probably has a general applicability in compact spectrometers with a broad spectral region and moderately high resolution. © 2012 Optical Society of America

OCIS codes: 300.6190, 090.2890, 120.4820, 050.1950.

1. Introduction

Spectrometers are widely applied for element analysis and content measurement in modern steel and iron, chemical, metallurgy, materials, and environment pollution domains, and so on. At present Rowland or Czerny–Turner configurations are the typical mounts in many spectrometers [1–8]. To obtain a high spectral resolution, long camera foci and high groove density gratings are usually used. Some Rowland and Czerny–Turner mounts utilized the scanned grating or several gratings to cover the broad spectral range [1–8]. The German Spectro Company has developed SPECTROLAB ARCOS, in which 32 line array CCDs and 2 gratings were used to cover a 130–770 nm region with 3 pm (130–340 nm) and 6 pm (340–770 nm) resolution [9]. However, long foci lead to a large volume of the instrument, and high groove density gratings limit the maximum diffraction range. Using many CCDs and several gratings increases the complexity of instrument. One solution is the Echelle spectrometer with multiple optical components [10], and another is the flat field concave holographic grating [11]. It is an important dispersion component that provides both dispersion and camera functions [12,13]. It is very suitable to integrate with a line array CCD to produce a spectrometer with a sole optical component. Because of the conflicts between broad spectral region and high resolution, it appears reasonable to design an optical system that has a broad spectral region and a low resolution or a narrow spectral region and a high resolution. For example, Yu *et al.* have proposed a design method for realizing a configuration with a resolution of 0.55 nm in the UV region 120 nm–180 nm [14]. Peng *et al.* have proposed to switch two gratings to broaden the spectral region [15]. In this paper, we also propose a simple method for solving the problem. Based on Namioka grating theory[12,13], common diffraction orders and simultaneous minimal aberration (CDO-SMA) are used to realize the broad spectral region and moderately

1559-128X/12/040509-06$15.00/0

high resolution in a flat field concave holographic grating configuration. A genetic algorithm (GA) and ZEMAX software are applied to realize these ideas. It is confirmed that the spectral region and resolution here are better than for the existing configuration based on flat field concave holographic grating. The principle of realizing a broad spectral region and a moderately high resolution is described in Section 2. The practical method for realizing this idea is described in Section 3. A near-normal-incidence example is given in Section 4. Conclusions are given in Section 5.

2. Principle of Realizing Broad Spectral Region and High Resolution

The schematic diagram of a flat field concave holographic grating is illustrated in Fig. 1 [12], and the Cartesian coordinate system of the grating also is denoted. The origin point, O, is on the grating vertex. The x axis is projected to origin point, and the y and z axes are perpendicular and parallel to the grooves of grating, respectively. The direction of the slit length is along the z axis. The irregular groove density of the concave holographic grating itself is described by the coordinates of two different construction points $C(r_C, z_C, \gamma)$ and $D(r_D, z_D, \delta)$, a construction wavelength λ_0, and the diffraction order m. $A(r, z, \alpha)$ is a point at the entrance silt, and A'_λ represents the diffraction foci of wavelength λ. $H(r_H, z_H, \beta_H)$ is the perpendicular point of the imaging plane. The coordinates w, and l are used only for the points on the grating, and $P(w, l)$ is any point on the grating.

Based on the concave grating theory of Namioka, The light-path function F of the ray APA'_λ is [12,13]

$$F = F_{000} + wF_{100} + lF_{011} + \frac{1}{2}w^2F_{200} + \frac{1}{2}l^2F_{020} + \frac{1}{2}w^3F_{300} + \frac{1}{2}wl^2F_{120} + \cdots\cdots . \quad (1)$$

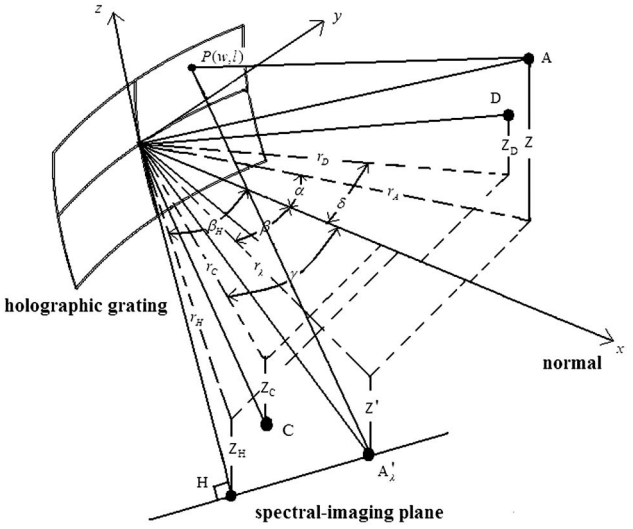

Fig. 1. Schematic diagram of the flat field concave holographic grating.

F_{ijk} is expressed in the form

$$F_{ijk} = M_{ijk} + \frac{m\lambda}{\lambda_0}H_{ijk}. \quad (2)$$

M_{ijk} represents the terms peculiar to mounting parameters, and H_{ijk} represents the terms peculiar to recording parameters. The explicit expressions M_{ijk} and H_{ijk} can be found in Ref. [12]. To realize a broad spectral region, we divide the spectral region into two parts, which are low spectral region (180–360 nm) and high spectral region (360–720 nm). First, we design a flat field concave holographic grating applied for the +2nd diffraction order and low spectral region (180–360 nm), and we also carry out aberration correction to obtain optimized mounting and recording parameters (M_{ijk}, H_{ijk}) for this grating. It could be considered that the grating could be applied in an optical configuration with narrow spectral region and moderately high resolution. Second, the flat field concave holographic grating is applied for the +1st diffraction order and high spectral region (360–720 nm). Because of the dependence of aberrations in the light path on $m\lambda$ alone, the mounting and recording parameters (M_{ijk}, H_{ijk}) are the same as those for the spectral region 180–360 nm. They appear as the following expression:

$$\begin{aligned} F_{ijk} &= M_{ijk} + \frac{2\lambda_{\text{low}}}{\lambda_0}H_{ijk} \\ &= M_{ijk} + \frac{\lambda_{\text{high}}}{\lambda_0}H_{ijk}(2\lambda_{\text{low}} = \lambda_{\text{high}}). \end{aligned} \quad (3)$$

This proves that the aberration correction of the +2nd order applies equally well to the +1st order. The entrance slit and imaging plane need not change, and the grating also is holding at the original position. In practical spectrometers, the preoptics assembly is usually used to lead light into the entrance slit from the light sources. Two high transmission bandpass filters can be used alternatively for selecting spectral region 180–360 nm and 360–720 nm, respectively. These filters can be used in parallel light paths to decrease the refraction influence on the imaging performance. At present both Newport and Thorlabs provide the services of all kinds of custom-built filters. It is also true that many advanced CCD detectors have realized high quantum efficiency in both the UV and visible spectral regions. The potential for high intensity is clear from the single diffraction element and the direct imaging on the CCD. A blaze holographic grating etched by ion beam etching technology may be advantageous for uniform intensity in two spectral regions [16]. Based on the description above, we would realize a broad spectral region, a moderately high resolution, and high intensity in a compact spectrometer based on a flat field concave holographic grating.

3. Design Method of the Flat Field Concave Holographic Grating

For simplification, the incidence and diffraction are defined in the x–y plane. Figure 2 shows a diagram of the Cartesian coordinate system of the grating. The surface of the grating blank is described as [12,13]

$$x = \sum_{i=0}^{\infty}\sum_{j=0}^{\infty} a_{ij} y^i z^j (a_{00} = a_{10} = 0, j = \text{even}). \quad (4)$$

Giving suitable values to the coefficients a_{ij}, we can obtain the expressions for spherical, toroidal, ellipsoidal, and other aspheric surfaces. In this paper, we consider a spherical mirror as the grating blank, and the expression [Eq. (4)] yields

$$x = a_{20} y^2 + a_{02} z^2 (a_{20} = a_{02} = 1/2R). \quad (5)$$

If we consider only the major influences on aberration, the light-path function F of ray APA'_λ could be described as

$$F = F_{000} + wF_{100} + lF_{011} + \frac{1}{2}w^2 F_{200} + \frac{1}{2}l^2 F_{020} + \frac{1}{2}w^3 F_{300} + \frac{1}{2}wl^2 F_{120}. \quad (6)$$

To guarantee diffraction light focusing on the imaging plane, the meridian imaging condition ($F_{100} = 0$) should be met:

$$m\lambda = \sigma(\sin\alpha - \sin\beta_\lambda), \quad (7)$$

where α is the angle of incidence and β_λ is the angle of diffraction in λ. σ is the effective grating constant, and m is the diffraction order. The spectral-imaging plane could be described as

$$r'_\lambda = \frac{r_H}{\cos(\beta_H - \beta_\lambda)}. \quad (8)$$

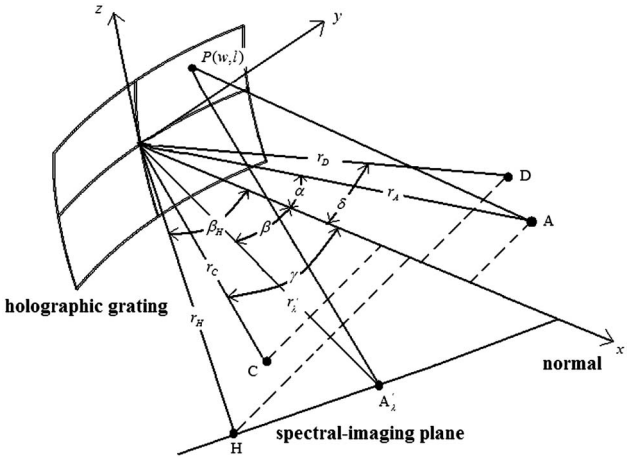

Fig. 2. Diagram of the Cartesian coordinate system of the grating in the x–y plane.

r_H is the perpendicular distance between the origin O and the imaging plane, and β_H is the angle between the x axis and the line OH. Table 1 gives the spectrometer parameters that should be determined before designing the flat field concave holographic grating. The diffraction angle β_λ and distance r'_λ in λ can be induced by Eqs. (7) and (8), respectively. Based on Namioka theory, the minimal-aberration function of the flat field concave holographic grating can be expressed as [12,13]

$$f[r, \alpha, r_H, \beta_H, a_{20}, r_C, z_C, \gamma, r_D, z_D, \delta] = \min \int_{\lambda_1}^{\lambda_2} (F_{200}^2 + F_{020}^2 + F_{300}^2 + F_{120}^2) d\lambda, \quad (9)$$

where mounting parameters are represented by $(r, \alpha; r_H, \beta_H)$ and recording parameters are represented by $(r_C, z_C, \gamma; r_D, z_D, \delta)$. a_{20} is used to calculate the radius of curvature of the grating blank by Eq. (5). It is apparent that those variables cannot be expressed by the analytic equation. It requires an optimized method that could be applied to obtain the initial mounting and recording parameters. To achieve this goal, we consider a GA that can be used to find the initial optimization parameters meeting the minimal-aberration function in Eq. (9). Goldberg has developed the GA for a further application [17], and the mature and reliable GA software toolbox has been integrated into MATLAB. It is possible for us to solve our problems by the MATLAB program, in which the initial population, objection function, and constrain function are written by us. The initial population includes variables needed for the problems to be optimized $(r, \alpha, r_H, \beta_H, a_{20}, r_C, z_C, \gamma, r_D, z_D, \delta)$. The objection function and constrain function are given by Eqs. (9) and (10), respectively [12,13]:

$$\sigma = \frac{\lambda_0}{(\sin\delta - \sin\gamma)} (\sin\delta > \sin\gamma). \quad (10)$$

4. Design Results and Analysis

Based on the requirements for the volume of the instrument and the resolution in our institute, we define the expected parameters of the spectrometers at the beginning of the spectral-imaging system design in Table 2 and give the initial population range used by GA in Table 3. After 50 iterations are finished, we

Table 1. Design Parameters of the Spectrometer

Parameters
Spectral region (diffraction order)
Spectral resolution
Entrance slit
Effective grating constant (or grooves/mm)
CCD pixel size
CCD effective pixel numbers

Table 2. Practical Parameters of the Spectrometer

Parameters	Value
Spectral region (diffraction order)	180–360 nm (+2nd), 360–720 nm (+1st)
Spectral resolution	0.2 nm @ (180–360 nm), 0.4 nm @ (360 nm–720 nm)
Entrance slit	1 mm (z direction) × 10 μm (y direction)
Effective grating constant (or grooves/mm)	1.389 μm (720 grooves/mm)
CCD pixel size	12 μm × 12 μm
CCD effective pixel numbers	4096 × 128

Table 3. Initial Population Range

Parameters	Value
r, α	100–130 mm, $-10° \sim 10°$
r_H, β_H	100–130 mm, $-10° \sim 10°$
a_{20}	0.001–0.01
r_C, γ	0–200 mm, $-50° \sim 50°$
r_D, δ	0–200 mm, $-50° \sim 50°$
z_C, z_D	0 mm

obtain the initial optimization parameters meeting the minimal-aberration function (9) and constrain function (10). We model an optical configuration based on the concave holographic grating in ZEMAX, and the initial optimization parameters are input to perform the second optimization based on the evaluation function of minimizing the spot diagram radius. The optimization variables are coordinates of mounting and constructing points. Tables 4 and 5 show the results optimized by GA and ZEMAX, respectively. Table 6 also gives the physical parameters of the holographic concave grating designed by us. Finally, we also verify our design results by light ray trace in ZEMAX. The single wavelength spot radius versus wavelength is applied to evaluate the aberration correction of the configuration based on our designed grating, and line-pair spectral images are applied to evaluate its resolution. Figure 3 shows the layout of the optical configuration based on the flat field concave holographic grating, and Figs. 4(a) and (b) show the single wavelength spot radius versus wavelength in two spectral regions. We can find

Table 6. Physics Parameters of the Holographic Concave Grating

Parameters	GA	ZEMAX
Grooves/mm	720 lines/mm	
Grating constant	$\sigma = 1.389$ μm	
Blaze wavelength	270 nm, 540 nm	
Entrance pupil diameter	20 mm	
Curvature radius of the grating blank	115.0726 mm	115 mm

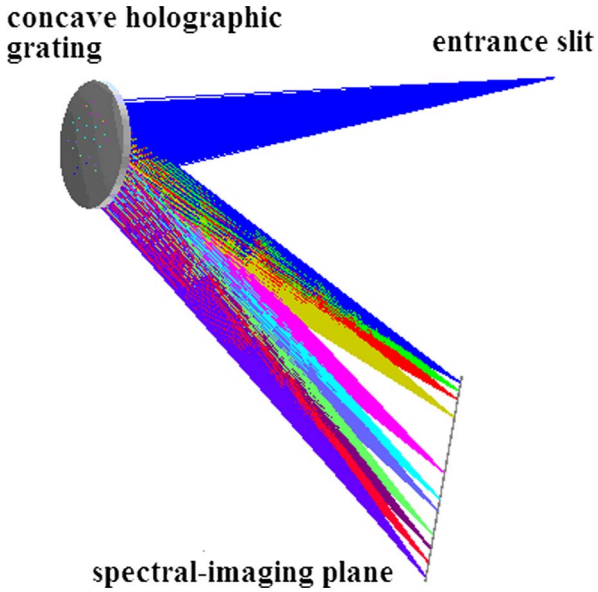

Fig. 3. (Color online) Layout of the optical configuration based on the flat field concave holographic grating.

that the RMS of each wavelength is kept around 20 μm, and no acute movement happens. The similar single wavelength spot radius versus wavelength in Figs. 4(a) and (b) also tells us that the same aberration correction is achieved in two spectral regions. Figure 5 shows a spectrum of line pairs imaged on the Line Array CCD in the 180–360 nm region. It shows that several simulation spectral lines are distinguished, and the magnified parts provide the resolution demonstration in the design wavelengths 180, 180.2, 282.4, 282.6, 359.8, and 360 nm. Figure 6 shows a spectrum of line pairs imaged on the line array CCD in the 360–720 nm region. It shows that

Table 4. Constructing Parameters of the Holographic Concave Grating

Parameters	GA	ZEMAX
Constructing point 1	$r_C = 112.9739$ mm, $\gamma = 24.5338°$	$r_C = 96.4332$ mm, $\gamma = 13.3633°$
Constructing point 2	$r_D = 141.7733$ mm, $\delta = 47.1538°$	$r_D = 106.0317$ mm, $\delta = 33.302°$
Constructing wavelength	0.4416 μm	
Diffraction order	+2nd order (180–360 nm); +1st order (360–720 nm)	

Table 5. Mounting Parameters of the Holographic Concave Grating

Parameters	GA	ZEMAX
Incidence point	$r = 125.3085$ mm, $\alpha = -9.9985°$	$r = 125.3$ mm, $\alpha = -10°$
Diffraction plane	$r_H = 110$ mm, $\beta_H = 5.9498°$	$r_H = 109.7483$ mm, $\beta_H = 6.779°$

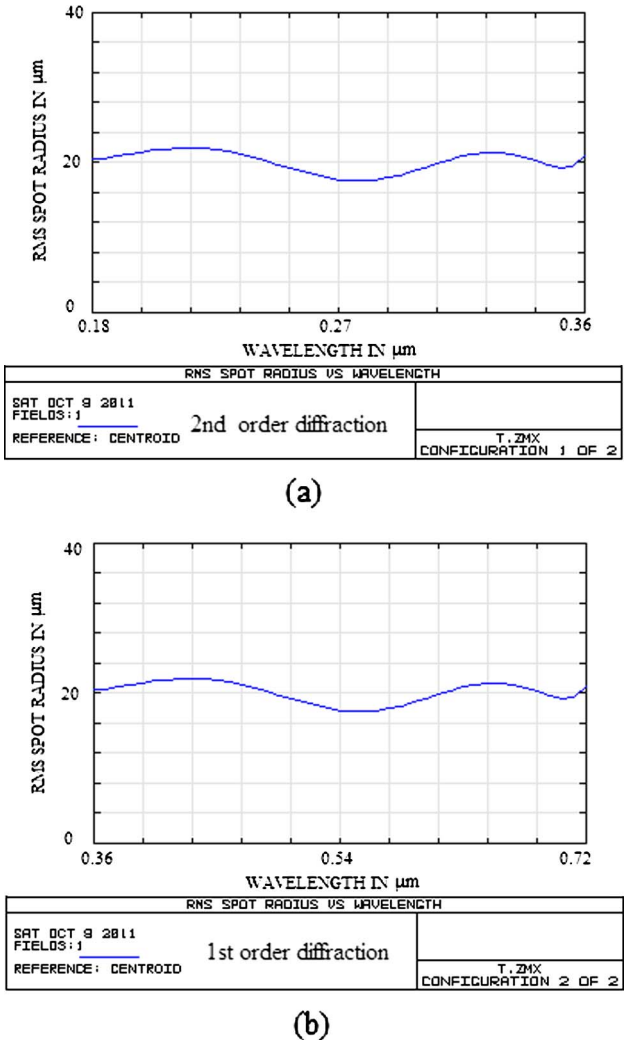

Fig. 4. (Color online) Single wavelength spot radius versus wavelength: (a) 180–360 nm, (b) 360–720 nm.

several simulation spectral lines are distinguished, and the magnified parts provide the resolution demonstration in the design wavelengths 360, 360.4, 564.8, 565.2, and 719.6, 720 nm. Based on the simulation analysis above, we can concluded, using filters to suppress the unwanted order, that this flat field holographic grating configuration can be used in the 180–720 nm broad region with a moderately high resolution. The spectrum of line pairs could be imaged on a bar line array CCD (45.125 mm × 1 mm), and the TDI camera C10000-601 (Hamamatsu Company) is appropriate for its imaging plane [18]. The performance of the flat field concave holographic grating is satisfied at the target.

5. Conclusion

We focus on the optimized design of a simple, broad spectral region, moderately high resolution, and high intensity flat field spectrometer for the visible and near-UV. The major new optical feature is the spectral overlap of 2nd and 1st orders at wavelengths of 180 to 360 nm and 360 to 720 nm, which is widely used to realize the purpose of a broad spectrum. The dependence of aberrations in the light path on $m\lambda$ alone is also taken into account, which enables optimization of one order to apply equally well to the other. Similarly, the resolving power ($\lambda/\Delta\lambda$) will be the same for both orders because of the same angles and light paths for a given $m\lambda$. To obtain moderately high intensity in both diffraction orders, we also proposed etching a blaze holographic grating by ion beam etching technology, which may be advantageous for a uniform intensity in two spectral regions. Based on the Namioka grating theory, we develop a practical design method of a flat field concave holographic grating with the help of GA and ZEMAX software. An example modeled in ZEMAX proved our ideas, in which the resolution reached 0.2 nm at 180–360 nm and 0.4 nm at 360–720 nm. In conclusion, we propose a simple method to solve the conflicts between broad spectral region and high resolution in a compact spectrometer based on a flat field concave holographic grating and line array

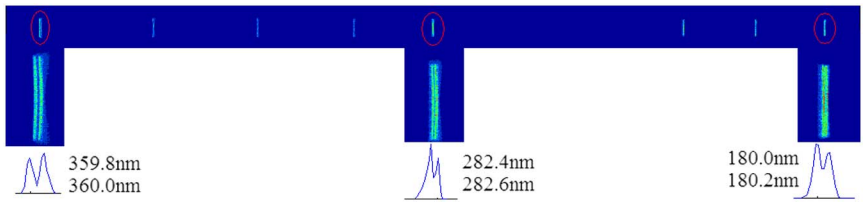

Fig. 5. (Color online) Spectrum of line pairs imaged on line array CCD in 180–360 nm.

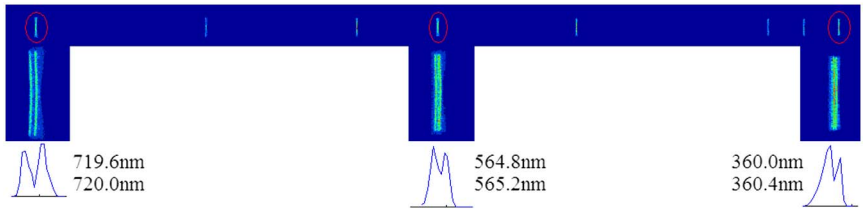

Fig. 6. (Color online) Spectrum of line pairs imaged on line array CCD in 360–720 nm.

CCD. Our ideas should be helpful for improving the performance of compact spectrometers.

This research is supported by the Central Institute of Iron & Steel Research (2011YQ140147-06) in Beijing.

References

1. M. P. Chrisp, "Aberrations of holographic toroidal grating systems," Appl. Opt. **22**, 1508–1518 (1983).
2. W. C. Cash, Jr., "Aspheric concave grating spectrographs," Appl. Opt. **23**, 4518–4522 (1984).
3. J. Simon, M. Gil, and A. Fantino, "Czerny-Turner monochromator: astigmatism in the classical and in the crossed beam dispositions," Appl. Opt. **25**, 3715–3720 (1986).
4. W. R. McKinney and C. Palmer, "Numerical design method for aberration-reduced concave grating spectrometers," Appl. Opt. **26**, 3108–3118 (1987).
5. R. Grange "Aberration-reduced holographic spherical gratings for Rowland circle spectrographs," Appl. Opt. **31**, 3744–3749 (1992).
6. R. T. Marsha and D. G. Torr, "Compact imaging spectrograph for broadband spectral simultaneity," Appl. Opt. **34**, 7888–7898 (1995).
7. D. R. Austin, T. Witting, and I. A. Walmsley, "Broadband astigmatism-free Czerny-Turner imaging spectrometer using spherical mirrors," Appl. Opt. **48**, 3846–3853 (2009).
8. Hettrick Scientific, "Hardware products," http://www.hettrickscientific.com/products.
9. SPECTRO, "SPECTRO ARCOS," http://www.spectro.com/pages/e/p010304.htm.
10. R. Tousey, J. D. Purcell, and D. L. Garrett, "An Echelle spectrograph for middle ultraviolet solar spectroscopy from rockets," Appl. Opt. **6**, 365–372 (1967).
11. Q. Zhou and L. F. Li, "Design method of convex master gratings for replicating flat field concave gratings," Spectrosc. Spectr. Anal. **29**, 2281–2285 (2009).
12. H. Noda, T. Namioka, and M. J. Seya, "Geometric theory of the grating," J. Opt. Soc. Am. **64**, 1031–1036 (1974).
13. T. Namioka, M. J. Seya, and H. Noda, "Design and performance of holographic concave gratings," J. Appl. Phys. **15**, 1181–1197 (1976).
14. L. Yu, S. Wang, Y. Qu, and G. Lin, "Broadband FUV imaging spectrometer: advanced design with a single toroidal uniform-line-space grating," Appl. Opt. **50**, 4468–4477 (2011).
15. P. Kong, Y. Ba, and W. H. Li, "Optimization of double-grating flat-field holographic concave grating spectrograph," Acta Opt. Sin. **31**, 0205001 (2011).
16. H. Lin and L. F. Li, "Fabrication of extreme-ultraviolet blazed gratings by use of direct argon-oxygen ion-beam etching through a rectangular photoresist mask," Appl. Opt. **47**, 6212–6218 (2008).
17. D. E. Goldberg, *Genetic Algorithms in Search, Optimization, and Machine Learning Reading* (Addison-Wesley, 1989).
18. Hamamatsu, "Image measurement cameras," http://jp.hamamatsu.com/en/product_info.